Polymer Degradation and Stability
December 2024, Volume 230, Pages 111025 (12p.)
https://doi.org/10.1016/j.polymdegradstab.2024.111025
https://archimer.ifremer.fr/doc/00915/102704/

Embrittlement induced by oxidation in polyethylene: Role of initial bimodality

Laot Robin [1, 2, 3, *], Le Gac Pierre Yves [2], Le Gall Maelenn [2], Broudin M. [1], Ovalle C. [3], Laiarinandrasana L. [3]

[1] EDF Lab Les Renardières, MMC, Avenue des Renardières, 77250 Écuelles, France
[2] IFREMER, Centre de Bretagne, 29280 Plouzané, France
[3] Mines Paris, PSL University, Centre for Material Sciences (MAT), CNRS UMR 7633, BP 87 91003 Evry, France

* Corresponding author : Robin Laot, email address : Robin.laot@minesparis.psl.eu

Abstract :

High density polyethylene films (200 µm) with an initial bimodal chain length distribution were aged in ovens at 60°C, 70°C, and 80°C. Oxidation effects were characterized at the macromolecular scale to measure the chain length distribution, the amount of crystalline phase, the type of crystallites, and the thickness of the amorphous layer. Additionally, mechanical properties were measured using tensile tests. Regardless of the aging temperature, the same behavior was observed: bimodal chain length distribution became unimodal, the crystallinity ratio increased, the amorphous layer thickness decreased, and the polyethylene became brittle. The embrittlement of the polymer is discussed, and two criteria are proposed: a critical molar mass and a critical amorphous layer thickness. The latter appears to be independent of the initial chain length distribution of the polyethylene.

Highlights

► Oxidation changes the chain length distribution from bimodal to unimodal. ► Oxidation leads to the embrittlement of the polymer. ► An embrittlement criterion can be defined for polyethylene. ► Critical amorphous layer thickness can describe embrittlement with a value of 7.5 ± 0.5 nm.

Keywords : Polyethylene, Bimodal, Embrittlement, Oxidation aging

1. Introduction

High density polyethylene (HDPE) is a commonly used polymer due to its low cost, ease of processing, and high elongation at break. It is also one of the most widely produced polymers globally [1]. However, particularly in highly technical applications, it has several limitations such as creep resistance, which refers to material's ability to resist deformation over time under constant loading. Existing data have shown that HDPE deforms significantly under load, leading to failure [2–6]. To prevent this creep, researchers have developed new HDPE formulations [7–11] that incorporate bimodal chain length distribution [12–15].

Bimodality in HDPE was first introduced in the 2000s [16] through a two-phase polymerization process that generates a distribution of macromolecular chains consisting of both short and long chains. Different catalysts such as chromium, Ziegler-Natta, or metallocene catalysts can be used to achieve the desired molar mass distribution [17,18]. This type of material combines the best properties of both low molecular weight fractions (rigidity, ease of processing, etc.) and high molecular weight fractions (mechanical strength, resistance to melting, etc.) [17,19–22]. HDPE with a bimodal chain length distribution is therefore highly desirable for demanding applications. However, the durability of this bimodal material and its potential for embrittlement caused by oxidation are not yet fully understood.

Polyethylene (PE) is a polymer whose properties undergo changes over time due to oxidation, as the presence of oxygen triggers an irreversible chemical reaction within the material. The chemical mechanisms of polyethylene oxidation are well known and have been extensively studied, particularly in terms of kinetics. This degradation leads to macromolecular processes such as chain splitting and crosslinking, with the former being the most significant. PE oxidation leads to a decrease in the molar mass of the material. This decrease in chain length increases macromolecular mobility at the local

level, resulting in a higher degree of crystallinity as well as a reduction in the length of the amorphous phase. One of the consequences of oxidation on the mechanical properties is polymer stiffening and embrittlement. Numerous studies have demonstrated that PE transforms from a ductile to brittle state during oxidation [3,17,23–25]. Research has shown that the transition from ductile to brittle behavior can be explained by the critical molar mass concept, M'_c [26]. If the average molar mass of the polymer exceeds M'_c, it will display ductile behavior, whereas a molar mass less than M'_c will result in brittle behavior. Previous studies have demonstrated that the M'_c value for PE is approximatively 70 kg/mol [26,27] and that it is not dependent on the initial molar mass of the polymer [17,26]. However, it is unclear whether the concept of critical molar mass can be applied in the case of a bimodal chain length distribution of PE. To answer this question, a PE with a bimodal chain length distribution was accelerated aged in ovens and then characterized at the macromolecular scale in terms of its chain length.

After describing the experimental details, the results are presented in two parts. First, changes at the macromolecular scale due to aging are considered using techniques such as gel permeation chromatography, small- and wide-angle X-ray scattering, and differential scanning calorimeter. Second, the mechanical changes in the stress-strain curve are described, and a macroscopic embrittlement criterion is chosen. It is important to note that the PE considered here is not stabilized so as to reduce the aging temperature and duration. Finally, a conclusion is proposed.

2. Materials and Methods

2.1. Material

The samples studied here are the model HDPE with a bimodal chain length distribution; this resin is classified as type PE100-RC by the PE100+ association. Moreover, to reduce the aging time, no additives were added to the formulation. Materials were supplied by INEOS as pellets and then processed by thermal compression to obtain 200 µm thick films.

Pellets were placed in the mold, heated to 150 °C at a heating rate of 8 °C/min, and then pressurized at 3 bar for 5 min. Finally, the temperature was reduced to room temperature at a rate of 13 °C/min under pressure (3 bar). A quality procedure was carried out to ensure that the material had not oxidized during this process and that it was homogeneous in terms of crystallinity, thickness, and mechanical properties. To ensure that the materials are not degraded during processing, the chain length distribution was measured before and after, and the results are similar. The main characteristics of the samples produced according to this method are summarized in Table 1.

Table 1: Main properties of the polyethylene films used in this study

Characteristics	Standard method	Value
Type of polyethylene		PE100-RC with a bimodal chain length distribution
Thickness		238 ± 10 µm
Crystallinity ratio	ISO 11357-2	64 ± 1 %
Melting temperature	ISO 11357-2	130 ± 1 °C
Temperature at the start of melting	ISO 11357-2	84 ± 2 °C
Oxygen induction time at 200 °C	ISO 11357-6	0.17 ± 0.03 min
Tensile modulus	ISO 37	1.40 ± 0.09 GPa
Yield stress	ISO 37	26 ± 1 MPa

Tensile elongation at break	ISO 37	682 ± 94 %
Tensile stress at break	ISO 37	38 ± 6 MPa

2.2. Thermo-oxidative aging

The aging of the material was carried out in temperature-controlled ventilated ovens (type UFB500 from the Memmert company) at three temperatures: 60 °C, 70 °C, and 80 °C. Particular attention was paid to the aging conditions. To ensure that the results obtained during the accelerated aging process could be extrapolated to service temperatures, the maximum temperature was limited to 80 °C, which is below the initial melting temperature of HDPE. Among others, this avoids temperature-induced microstructural changes that have already been observed in other studies [28–31]. The use of low temperatures with reasonable aging times was possible thanks to the HDPE model and its formulation without added stabilizers. In addition, for the three aging conditions under investigation, due to the use of 200 µm thin films and temperatures below 100 °C, oxidation was homogeneous across the thickness. In other words, there was no diffusion-limited oxidation effect in this study.

2.3. Gel permeation chromatography

Gel permeation chromatography (GPC) was used to measure the chain length distribution and its evolution with aging. Samples of about 20 mg were dissolved in stabilized trichlorobenzene for 2 hours at 160 °C. They were then injected at 150 °C into a set of two 8.0 mm x 300 mm Agilent Mixed-B ID columns at a flow rate of 1 ml/min. A differential reactive index detector was used to perform the detection. Calibration was carried out in advance with polystyrene over a molar mass range from 500 to 8,000,000 g/mol. Chain length data were fitted with a single or double Gaussian distribution using Origin® software. Details are provided in the Results section below.

2.4. Differential scanning calorimeter

Differential scanning calorimeter (DSC) measurements were performed using a Q200 device (TA instrument) according to ISO 11357-2 [32]. Testing was performed under a nitrogen flow (50 ml/min) at a rate of 10 °C/min. Three samples were tested per condition using 5-10 mg of material. The crystallinity ratio was calculated using Equation 1:

$$\chi_C = \frac{\Delta H_f}{\Delta H_f{}^0} \qquad \text{(Eq 1)}$$

Where χ_C is the crystallinity ratio, ΔH_f is the measured melting enthalpy (J/g), and $\Delta H_f{}^0$ is the melting enthalpy of a fully crystalline PE and taken to be equal to 293 J/g [33,34].

2.5. X-ray measurements

Small- and wide-angle X-ray scattering (SAXS/WAXS) measurements were performed on a Xeuss 2.0 apparatus (Xenocs) equipped with a micro source using Cu Kα radiation (λ =1.54 Å) and point collimation (beam size: 300 × 300 µm²). The sample-to-detector distance, around 15 cm for WAXS and 1.5 m for SAXS, was calibrated using silver behenate as the standard. Through-view 2D diffraction patterns were recorded on a Pilatus 200k detector (Dectris). Integrated intensity profiles were computed from the 2D patterns using Foxtrot® software. The long period was computed using Equation 2.

$$L_p = \frac{2\pi}{q_{max}} \qquad \text{(Eq 2)}$$

Where L_p is the long period (nm) and q_{max} (nm) the maximum of the correlation peak.

The amorphous layer thickness was defined by Equation 3 from the long period L_p (previously defined using Equation 2 from SAXS measurements), and the crystallinity ratio (from DSC measurements) was defined using Equation 4.

$$l_a = L_p - l_c \quad \text{(Eq 3)}$$

$$l_c = \chi_c \frac{L_p \rho_a}{\rho_c - \chi_c (\rho_c - \rho_a)} \quad \text{(Eq 4)}$$

Where l_a and L_c are respectively the amorphous and crystalline layer thicknesses (nm), and ρ_a and ρ_c are respectively the amorphous and crystalline phase density (g/cm^3) taken to be equal to 0.863 and 0.997 g/cm^3 [35].

2.6. Tensile testing

Tensile testing was carried out on an Instron 5966 machine at 21 ± 2 °C and 50 ± 5 % relative humidity. Testing was performed on dumbbell specimens at a constant displacement rate equal to 10 mm/min. Test specimens are type 3 according to ISO37 [36] and obtained by die cutting. Three samples were tested per condition so as to ensure the reproducibility of the result. The force was measured with an Instron 500 N load cell, and the strain was obtained with an Instron AVE2 video extensometer. Engineering strain and stress were reported, while no corrections were made for thickness or width changes induced by necking.

3. Results

3.1. Changes at the macromolecular scale during aging

During oxidation, both crosslinking and chain scission occur within the amorphous phase of polymers [37,38]. To quantitatively characterize these processes, GPC measurements were performed. Results obtained for PE aged at 60 °C, 70 °C, and 80 °C are presented in Figures 1a, 1b, and 1c, respectively. Three main comments can be made based on these results. First, an increase in elution time is observed with aging, which indicates that chain scission is the predominant process during oxidation. This behavior is in accordance with current knowledge of the oxidation of PE with a unimodal chain length distribution [39–41]. Second, a change occurs in the shape of the curve. In the initial state, there are two distinct peaks that tend to form a single peak during aging. In other words, the bimodality of PE tends to disappear during oxidation, suggesting that longer chains are more sensitive to oxidation than shorter ones. The origin of this behavior is still under investigation. Finally, the transition from bimodal to unimodal distribution is observed for all the temperatures considered in this study (i.e., 60 °C, 70 °C, and 80 °C).

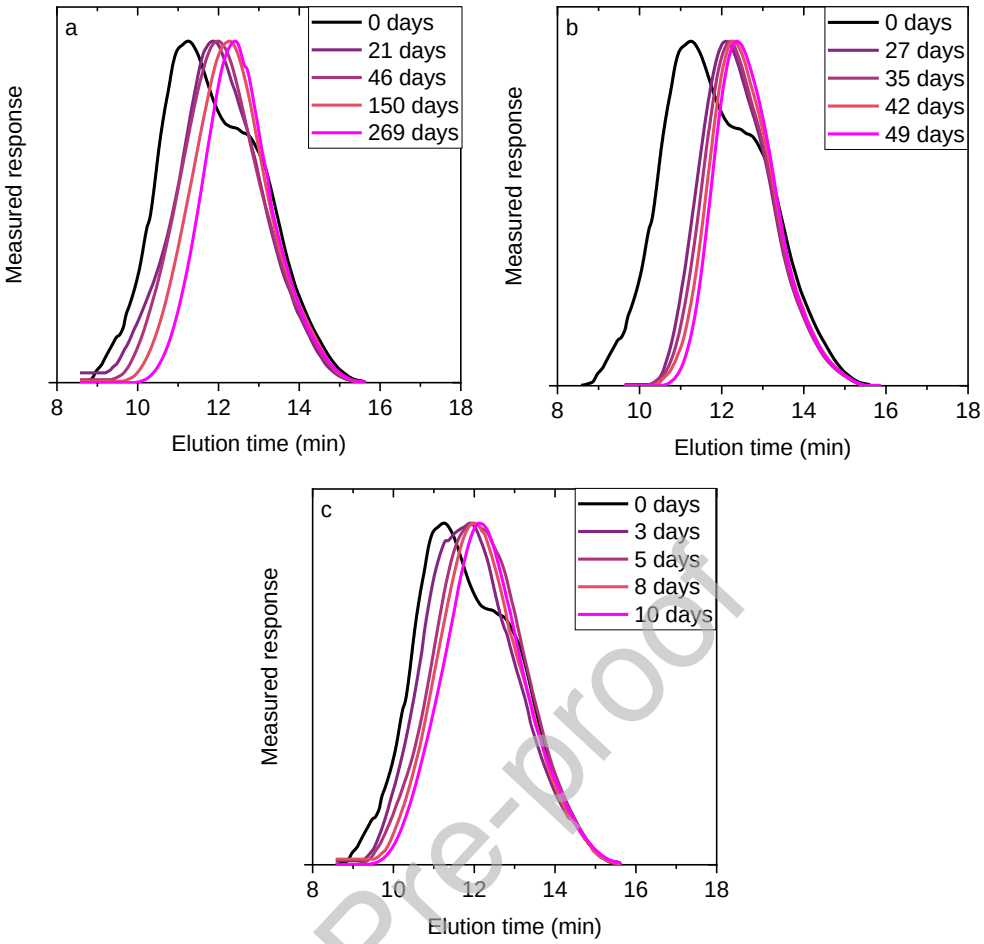

Figure 1: GPC results obtained after aging for polyethylene with a bimodal chain length distribution at 60 °C (a), 70 °C (b) and 80 °C (c)

The analysis of GPC results generally allows us to define three characteristic quantities relating to the chain length of a polymer, namely molar mass by number (M_n), molar mass by weight (M_w), and polydispersity index (Ip) [42,43]. Here results are polystyrene equivalent. In the case of a bimodal polymer, defining these quantities is complex, as the chain length distribution cannot be described by a single Gaussian curve. It is therefore necessary to fit the curves using several Gaussians, two in our case as shown in Figure 2a. During aging, the chain length changes, and the fit can be achieved by a single peak, showing a transition from bimodal to unimodal. For example, Figure 2b shows the curve fit for a 5-day aging period at 80 °C, while considering a bimodal distribution (two Gaussians, blue curve) and a unimodal distribution (one Gaussian, red curve); in both cases, the R^2 factor exceeds 0.99. In the following, we arbitrarily consider that an aged sample has a unimodal chain distribution when the curve can be fitted using a single Gaussian with a coefficient of determination greater than 0.99. It is thus possible to define a value of M_w as a function of aging time as shown in Figure 3. These results will be used to define an embrittlement criterion in the Discussion section.

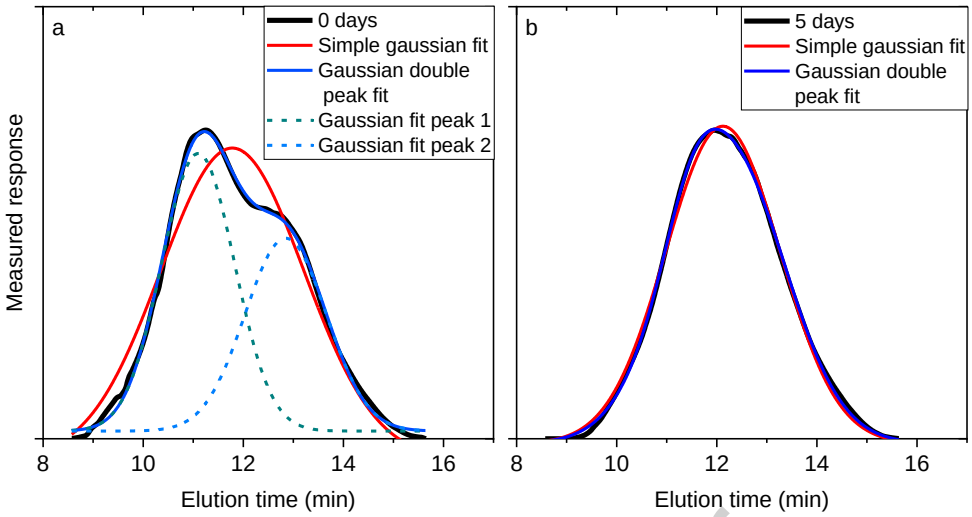

Figure 2: Data fitting of gel permeation chromatography results for unaged polyethylene (a) and polyethylene aged for 5 days at 80 °C (b)

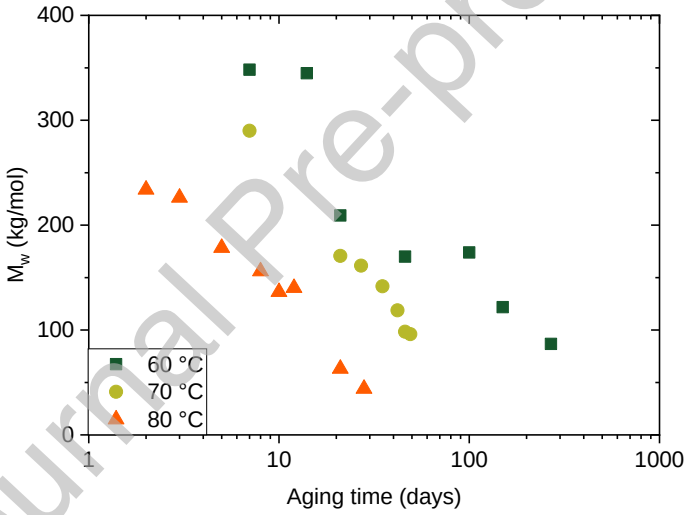

Figure 3: Changes in M_w during aging at 60 °C, 70 °C, and 80 °C for polyethylene with an initial bimodal distribution (M_w is only calculated when gel permeation chromatography results can be described using a single Gaussian curve with a R^2 factor above 0.99)

This section focused on an experimental description of the macromolecular changes that occur during the oxidation of PE with an initial bimodal chain length distribution. As expected, the process of chain scission predominates. Moreover, it becomes clear that the chain length distribution is modified by oxidation in the case of PE with an initial bimodal distribution. In the next section, we will assess the impact of aging on the microstructure of polymers.

3.2. Changes in the microstructure during aging

PE is a semicrystalline polymer with a crystalline phase that can be affected by oxidation. This part of the study focuses on the nature and amount of crystalline changes during aging.

First, we consider the nature of crystallites for which WAXS was conducted. Figure 4 shows the results for PE obtained with the bimodal chain length distributions in the initial state. Two distinct peaks at values of 2θ equal to 22° and 24° were observed for PE samples, respectively corresponding to the 110 and 200 orthorhombic reflections according to the Miller indices. It therefore appears that no change occurs in the crystalline nature of the polymers during aging.

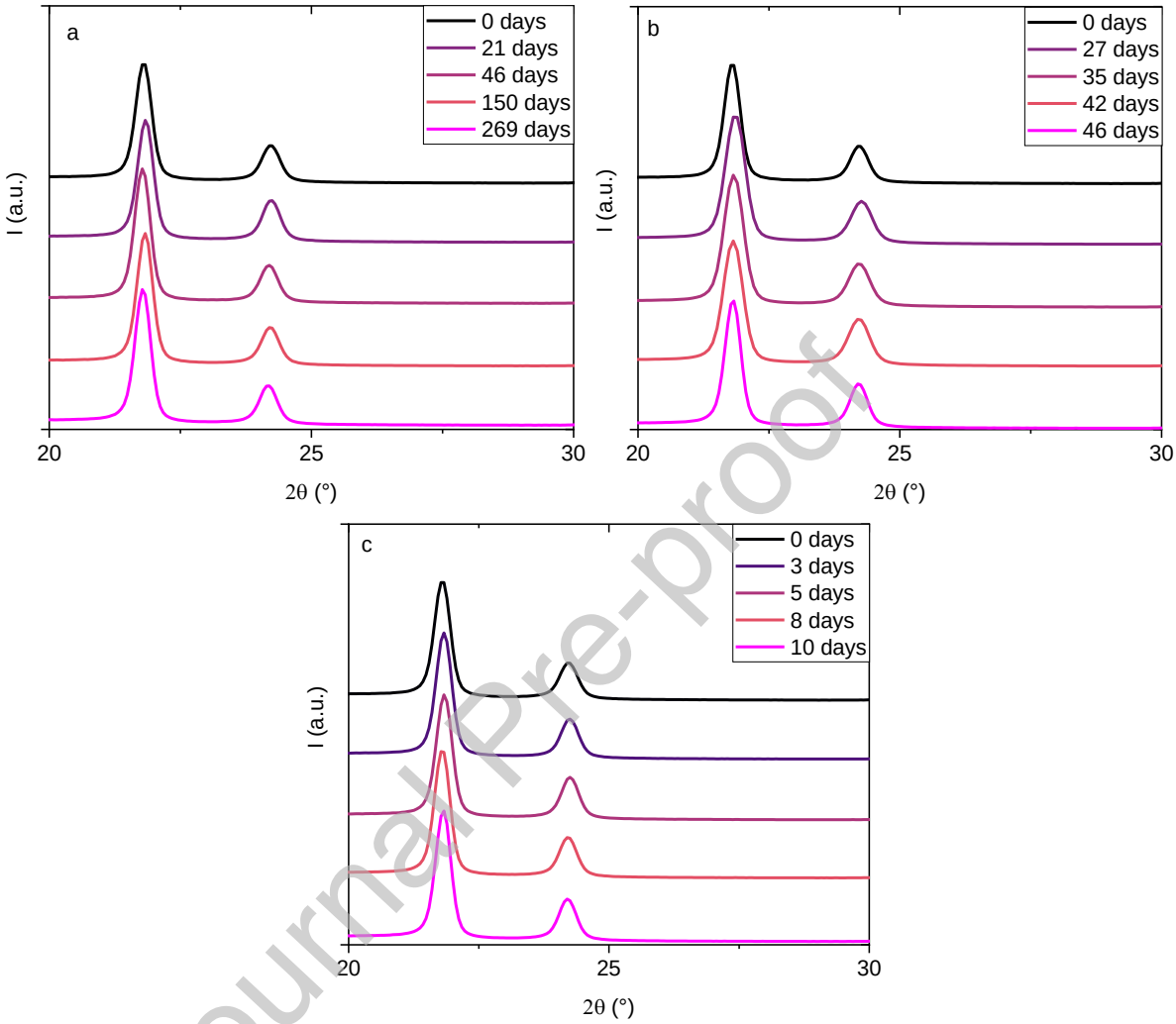

Figure 4: Wide-angle X-ray scattering results obtained after aging for polyethylene with an initial bimodal chain length distribution at 60 °C (a), 70 °C (b), and 80 °C (c)

Second, the amount of the crystalline phase is considered. To investigate changes in the crystallinity ratio in the material during aging, DSC tests were performed. Figure 5 shows the thermograms obtained during aging at 60 °C, 70 °C, and 80 °C. Results indicate that the melting temperature for unaged material is approximately 130 ± 1 °C. Slight increases in the melting temperature can be noted due to the fact that the chain length decreases with aging. By integrating the DSC signal, it is possible to measure the amount of the crystalline phase in the polymer. Figure 6 depicts the clear increase in the crystallinity ratio during oxidation. As an example, the initial crystallinity ratio is equal to 64 ± 1% in the unaged material and increases up to 73 ± 3% after 12 days of oxidation at 80 °C. This increase is well known in the literature and can be explained by the chemi-crystallization process observed numerous times in PE [17,44]. It can be described by the fact that due to the chain scission process, the chain length decreases. This decrease leads to an increase in macromolecule mobility, which allows the macromolecules to be integrated into the crystalline phase, thus leading to an increase in the

crystallinity ratio. It is worth noting that no changes in crystallinity ratio is observed when the polymer is aged under vacuum meaning that the observed increase in crystallinity is not related to a potential annealing of the PE.

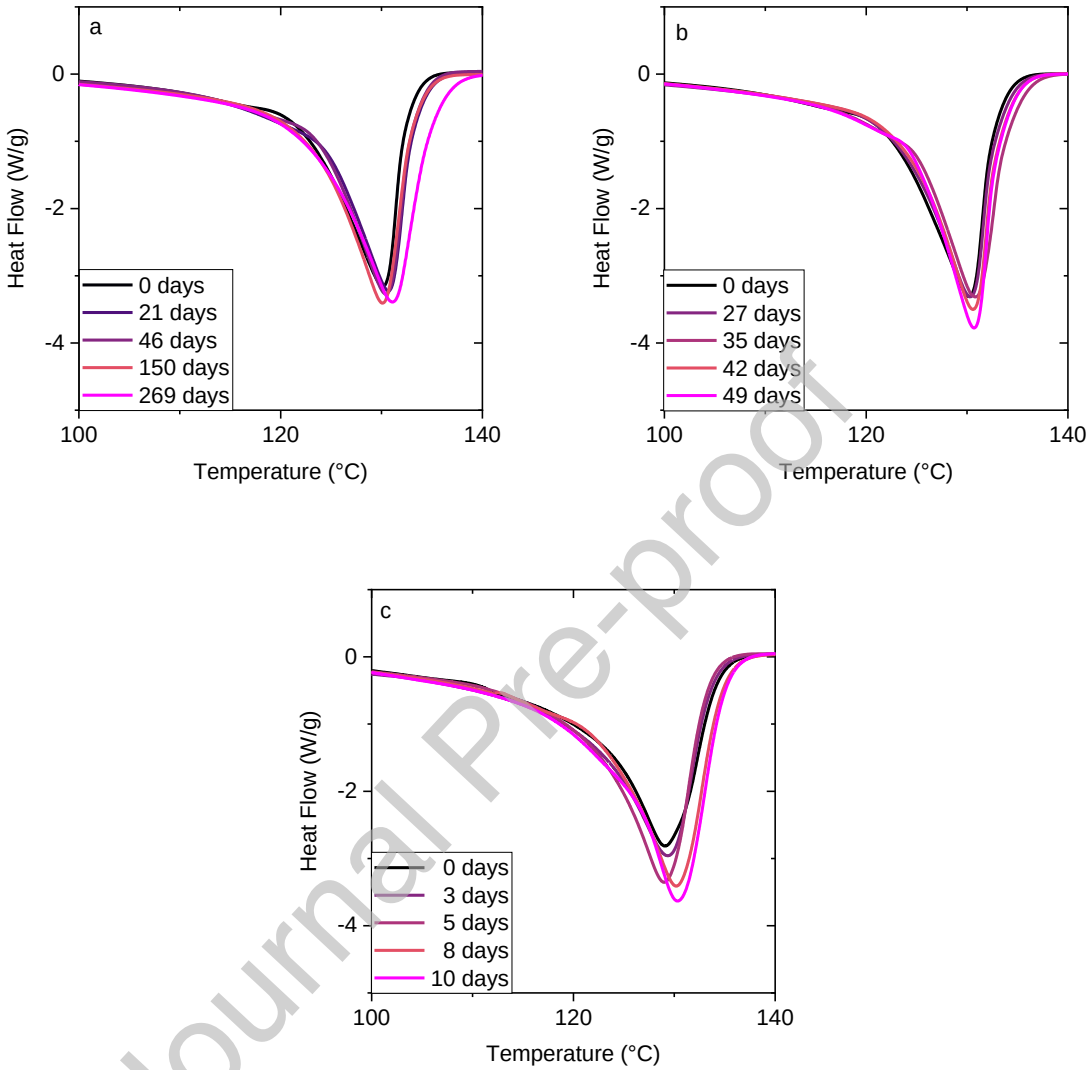

Figure 5: Differential scanning calorimeter results obtained after aging for polyethylene with an initial bimodal chain length distribution at 60 °C (a), 70 °C (b), and 80 °C (c)

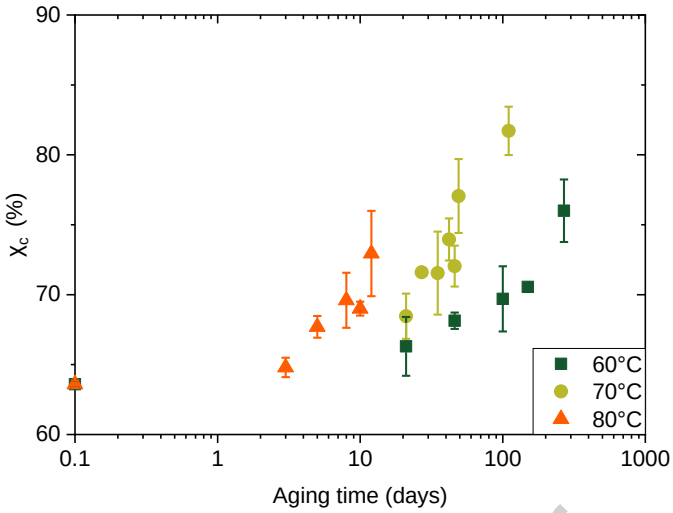

Figure 6: Changes in the crystallinity ratio (χ_c) at 60 °C, 70 °C, and 80 °C for polyethylene with an initial bimodal distribution as a function of aging time

Finally, we focus on the thickness of the amorphous layer (l_a), as it is known that variations in crystallinity levels can reduce the amorphous phase in PE during oxidation. To do so, SAXS tests were carried out. Changes in the thickness of the amorphous phase during aging are shown in Figure 7. During oxidation, and regardless of the aging temperature considered here, a decrease in the thickness of the amorphous phase is observed. As an example, the thickness of the amorphous layer decreases from 10.5 nm to 7 nm after 42 days of aging at 70 °C. The SAXS results clearly show that oxidation leads to a decrease in the thickness of the amorphous phase.

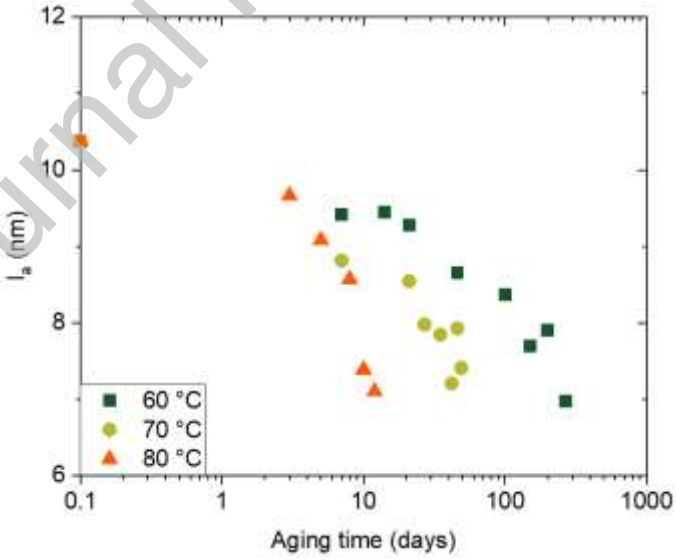

Figure 7: Changes in the amorphous layer thickness (l_a) at 60 °C, 70 °C, and 80 °C for polyethylene with an initial bimodal distribution as a function of aging time

The aim of this section was to characterize changes in the PE microstructure during oxidation based on three main parameters: the nature of the crystalline phase, the crystallinity ratio, and the thickness of the amorphous layer. It is clear that the initial bimodal chain length distribution does not modify the changes of the PE microstructure during oxidation. Regarding PE with a unimodal chain length

distribution, we did not observe any changes in the nature of the crystallites. However, we highlighted an increase in the degree of crystallinity due to the chemi-crystallization process, thus leading to a reduction in the thickness of the amorphous phase. The next section is dedicated to the mechanical properties of the PE and, more especially, to the embrittlement induced by oxidation.

3.3. Changes in engineering stress-strain curves induced by oxidation

The mechanical response of PE film is characterized here using a uniaxial tension test. Let us first focus on the results obtained for the unaged bimodal PE. The engineering stress-strain curve in Figure 8 can be described as follows:

- Initially, a linear and elastic part is observed. Young's modulus is determined at this stage.
- Then a deviation from linearity occurs with increasing stress up to a maximum (①) defined as the yield stress σ_y. The corresponding strain noted as ε_y was measured.
- After the yield stress, the stress decreases, and the deformation becomes heterogeneous due to the formation of a neck in the specimen (②). Necking propagation occurs, and the stress remains almost constant while the nominal strain increases.
- Under large strain, it is interesting to note that an instability occurs between points ③ and ④, which can be attributed to the appearance of a second necking in the sample during the tensile test. This second necking leading once again to a decrease in the engineering stress
- From a strain above 500%, the engineering stress increases again, and structural hardening takes place until specimen failure. Stress and strain at break can be measured, noted respectively as σ_b and ε_b.

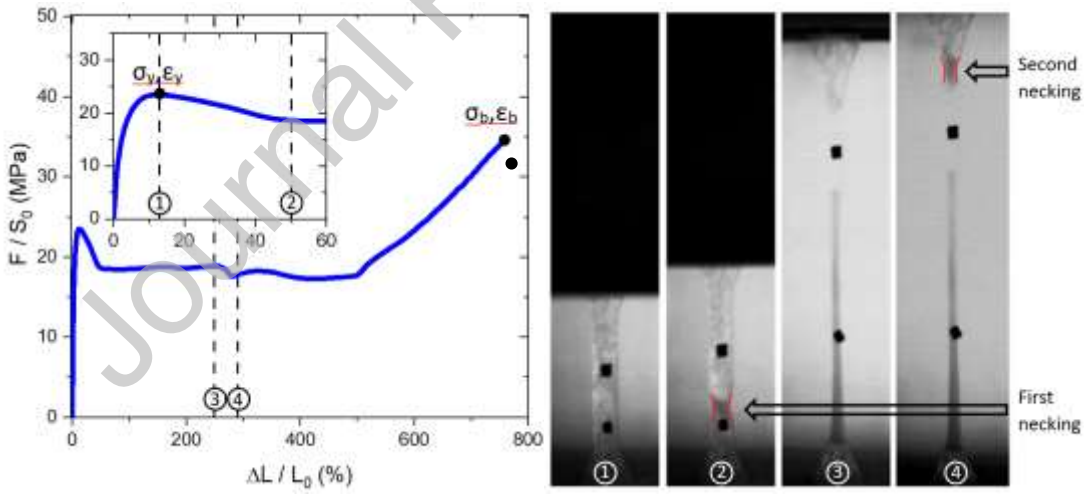

Figure 8: Stress-strain curve for the initial bimodal polyethylene

The stress-strain curve described above resembles that of material with an initial unimodal distribution [45].

As the polyethylene is deformed, the high molecular weight chains are stretched and align along the direction of the applied stress. Due to their long chain lengths, these high molecular weight chains create a highly entangled network that resists further deformation, leading to strain hardening. This network strengthens under strain, making it harder for the material to continue deforming.

Oxidation leads to modifications in the profile of the tensile stress-strain curve of the polymers. Figure 9 presents typical stress-strain curves obtained as a function of the aging times at 60 °C, 70 °C, and 80 °C. For the sake of readability, the abscissa scales are not the same in order to accommodate the mechanical responses during aging. It is observed that for each aging temperature, the structural hardening gradually decreases with an increasing aging time. In addition, strain at break decreases. For the longest aging times, no necking occurs in the sample, and the stress and strain at break are close to the yield (Figures 9e, 9j, 9o). This phenomenon may be explained by the decrease in the tie molecules. In fact, as oxidation occurs, chain scissions occur in the amorphous phase, leading to a decrease in the concentration of the tie molecules. At a significant stage of oxidation, the stress can no longer be transferred to the crystallites via the amorphous phase [7,10].

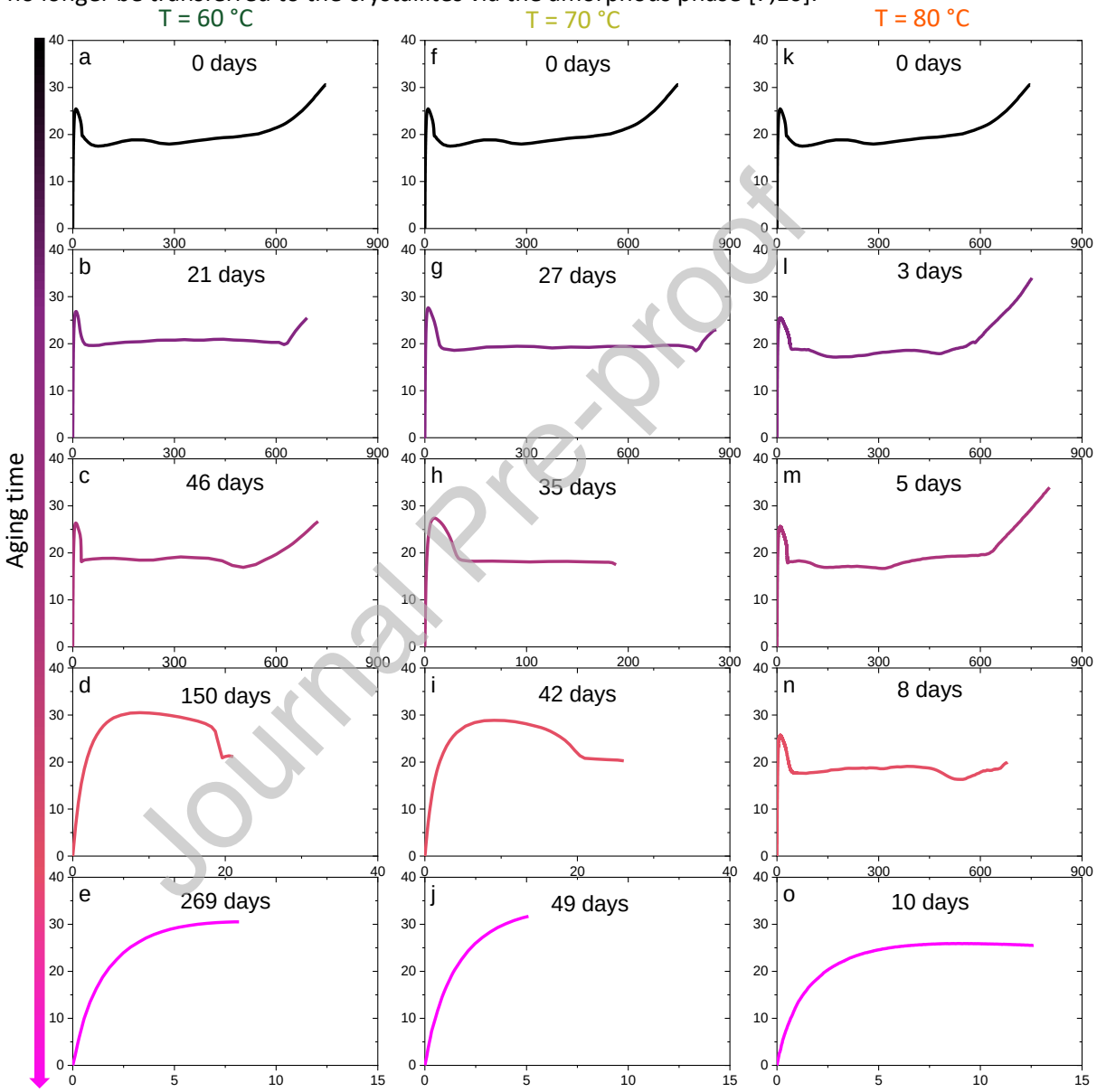

Figure 9: Stress (in MPa) as a function of the strain (%) curve for polyethylene with an initial bimodal distribution aged at 60 °C (a,b,c,d,e), 70 °C (f,g,h,i,j), and 80 °C (k,l,m,n,o)

Figure 10 depicts the variation in Young's modulus as a function of aging time for the three specified temperatures: 60, 70, and 80°C. It can be observed that the modulus exhibits an increase with aging at all temperatures.

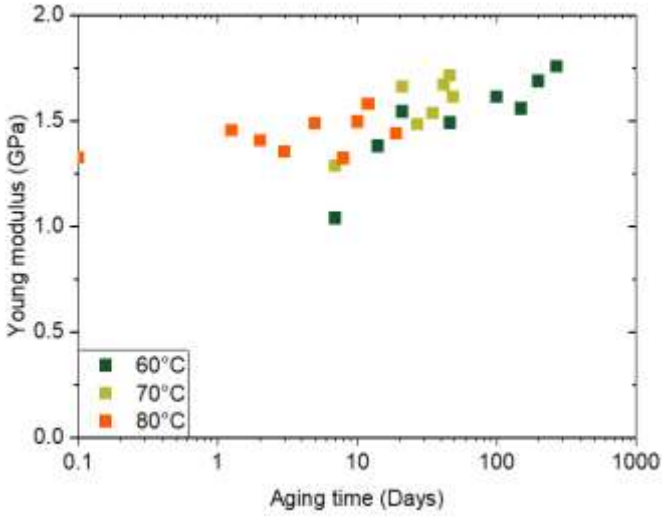

Figure 10: Evolution of the Young's modulus as a function of aging time for polyethylene aged at 60 °C, 70 °C, and 80 °C

Figures 11a and 11b illustrate the increase in Young's modulus and yield stress, respectively, as a function of the crystallinity ratio. An increase in Young's modulus is observed with the increase in the crystallinity induced by the degradation process. This increase can be described using an empirical mixing rule, such as the following:

$$E = E_c X_c + E_a(1 - X_c)$$

where E is the modulus of the polyethylene, X_c is the crystallinity ratio of the polymer, E_a is the modulus of the amorphous phase fixed at 40 MPa[46], and E_c is the modulus of the crystalline phase, which is determined (determined to be around 2.1 GPa.

Considering now the yield stress, as illustrated in Figure 11b, a slight increase is observed with the increasing crystallinity ratio. The interpretation of these results is challenging. However, it is worth noting that a linear relationship between yield stress and crystallinity ratio was previously demonstrated by Humbert et al. for polyethylene[47].This relationship has been explained by the fact that X_c represents the product of crystallite thickness and the stress concentration on the crystallites due to stress transmitters.

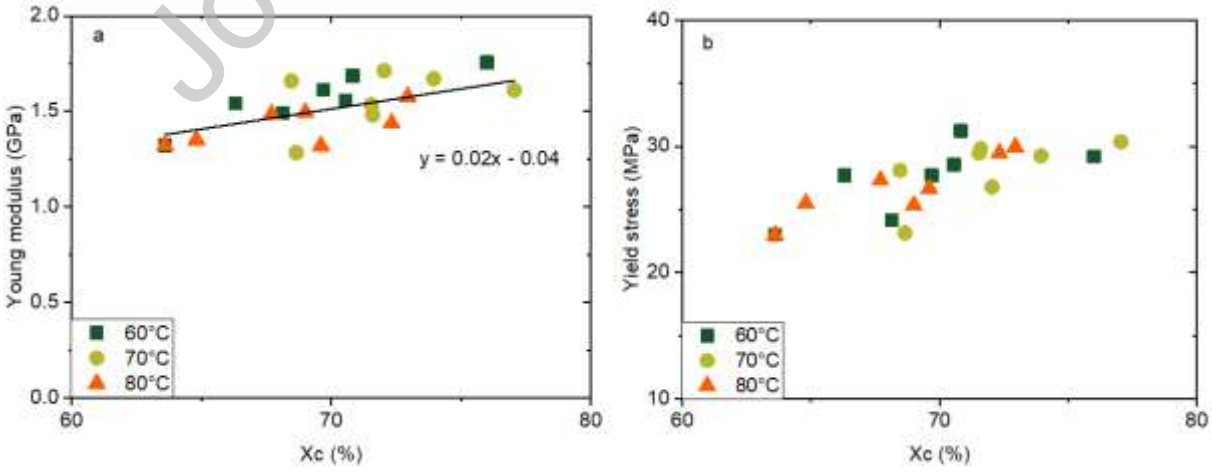

Figure 11: Evolution of the Young's modulus (a) and Yield stress (b) as a function of the crystallinity ratio X_c

Considering the mechanical changes in the stress-strain curve, several transitions appear to occur in the characteristics during aging.

3.4. Choice of macroscopic embrittlement criterion

A common method used when studying embrittlement is stress monitoring. According to Brown [48], ductile failure is observed when $\sigma_y > \sigma_b$ and brittle failure when $\sigma_y = \sigma_b$. Thus, the transition between ductile and brittle failure is the first point when σ_y and σ_b are equal. After this transition, the failure becomes brittle. In Figure 12, the ratio between yield stress and stress at break as a function of aging time is plotted. According to Brown, the points with an ordinate less than or equal to 1 are not ductile.

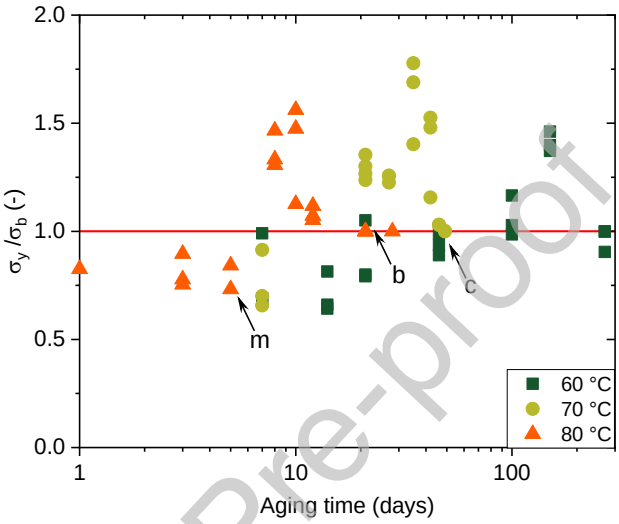

Figure 12: Evolution of the ratio between yield stress and stress at break as a function of aging time for polyethylene aged at 60 °C, 70 °C, and 80 °C

However, in this study, ductile failure with a large difference between ε_y and ε_b and a stess ratio near to or less than 1 can be observed for different curves as in Figures 9b, 9c, and 9m and identified in Figure 12. Indeed, the material undergoes hardening at the end of the test. Therefore, to overcome this ambiguity and obtain an embrittlement criterion, both stress and strain should be considered.

For this purpose, the ratio between yield stress and stress at break as a function of the ratio between yield strain and strain at break is plotted in Figure 13. The horizontal red line is Brown's condition of brittleness. The vertical red line corresponds to failure strain equal to yield strain. It is not possible to go beyond this line, because failure strain obviously represents the maximum strain possible. Inspired by Figure 9, the stress ratio (σ_y/σ_b) between 0.8 and 1.2 and strain ratio ($\varepsilon_y/\varepsilon_b$) between 0.77 and 1 are defined as a brittle area. In this study, 12 points are in this area, represented by hollow points in the different graphs below.

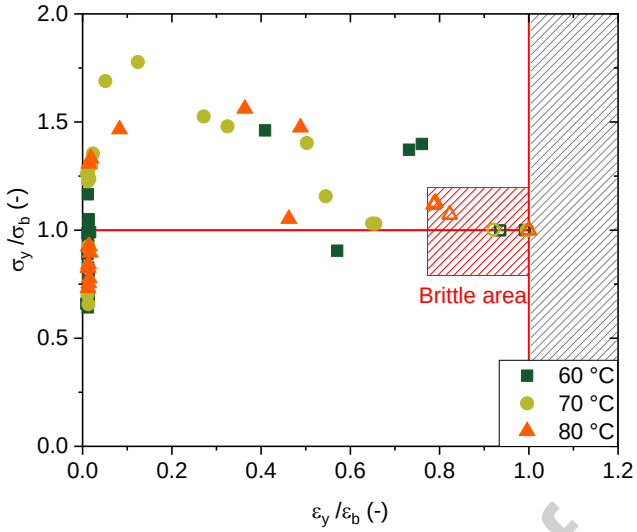

Figure 13: Ratio between yield stress and stress at break as a function of the ratio between yield strain and strain at break for polyethylene aged at different temperatures and aging times

During aging, we first observe an increase in the stress ratio up to a maximum without any changes in the strain ratio. This is followed by a decrease in the stress ratio down to 1 and fluctuations around it when the strain ratio tends toward 1. Therefore, the material tends toward the brittle zone with aging. The strain ratio seems to be a pertinent parameter to identify embrittlement. Consequently, in this study, the embrittlement criterion is only defined in terms of the strain ratio.

Figure 14a plots the strain ratio as a function of aging time for the three temperatures studied here. In the case of aging at 60 °C, the strain ratio is close to zero up to 100 days. At this point, the ratio increases dramatically and reaches the embrittlement zone. The same behavior is visible for other aging temperatures after different durations.

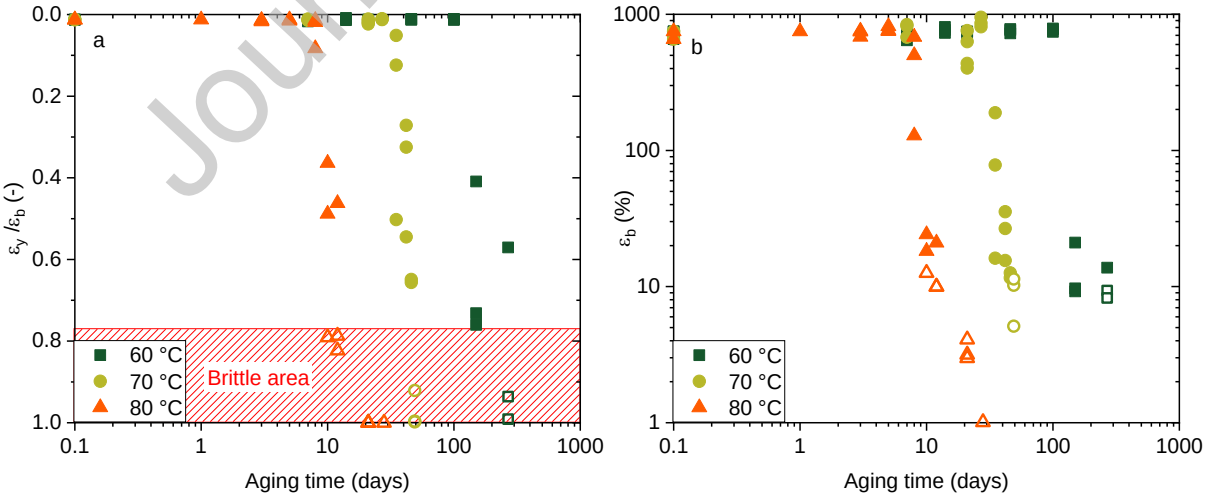

Figure 14: Evolution of strain ratio (a) and strain at break (b) as a function of aging time for polyethylene aged at 60 °C, 70 °C, and 80 °C

Due to the hyperbolic tangent curve, a characteristic embrittlement time can be defined for each aging temperature. Table 2 shows the characteristic ductile/brittle transition times obtained for the different temperatures studied. The values are obtained by determining the time required to obtain a strain ratio equal to 0.77 by linear regression for the rapidly increasing part.

Table 2: Characteristic ductile/brittle transition times obtained for the different temperatures studied

Aging temperature (°C)	60	70	80
Characteristic ductile/brittle transition times (days)	240	47	12

Figure 14b shows failure strain, instead of strain ratio, plotted as a function of aging time. The same data appear in Figures 14a and 14b, but they are presented in a different way with the hollow points representing the brittle failures. The trends for strain ratio and strain at break during aging appear similar. In the second case (Figure 14b), it can be established that embrittlement occurs when ε_b is less than or equal to 10%.

In the literature, some authors [17,37,49] use drop-in strain at failure as an embrittlement criterion. This criterion will be used to compare our results from the material with an initial bimodal distribution to those of the unimodal material.

To conclude this section on the effect of oxidation on the stress-strain curve of a PE with a bimodal chain length distribution, it is clear that degradation leads to significant changes in the failure characteristics: the PE changes from a ductile to brittle response for all temperatures considered in this study. An embrittlement criterion was established using strain ratio for the PE aged in this study. The remaining question is to define a criterion that is independent of the aging conditions to predict the embrittlement of the PE, which would allow for lifetime predictions.

4. Discussion

During oxidation, bimodal PE failure changes from ductile to brittle. This paper aims to evaluate macromolecular criteria to describe this mechanical embrittlement, which should be independent of the aging temperature and the initial chain length distribution.

4.1. Critical molar mass

The embrittlement of semi-crystalline polymers is often described by a critical molar mass (M'_c) defined as follows: when the polymer molar mass is greater than M'_c, the polymer exhibits ductile behavior, but when the molar mass is less than M'_c, it can exhibit brittle behavior.

According to Figure 15a, which plots strain ratio as a function of polymer molar mass for the three studied temperatures, there appears to be a critical molar mass for PE with an initial bimodal chain length distribution. In particular, when M_w is above 150 kg/mol, the strain ratio is less than 0.1, indicating ductile failure. When M_w is close to 100 kg/mol, the failure tends to be brittle. This study defines a critical molar mass of about 100 kg/mol for the PE considered.

To compare the values of M'c between the unimodal distribution and the initial bimodal distribution, it is necessary to use strain at break as the embrittlement criterion. Figure 15b shows the result of this study and the literature points for unimodal distribution PE [25]. It is clear that both materials have a critical molar mass. However, a difference in value is observed. For PE with an initial unimodal chain length distribution, the M'c value is about 70 kg/mol, while for PE with an initial bimodal chain length

distribution, the M'c value is about 100 kg/mol. In fact, the critical molar mass depends on the initial chain length distribution of the polymer.

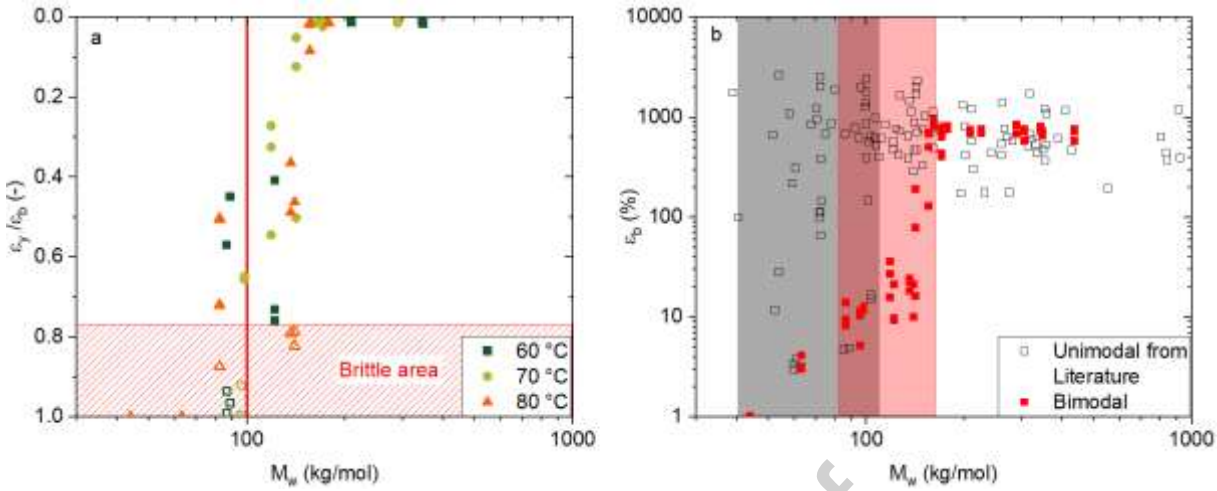

Figure 15: Determining the critical molar mass based on strain ratio (a) and strain at break compared with existing data from the literature[26] (b)

4.2. Amorphous layer thickness

Another parameter commonly used to describe polymer embrittlement during aging is the amorphous layer thickness. As chain scission occurs in the amorphous phase of the polymer during aging, there is an increase in chain mobility, resulting in an increase in the crystallinity ratio and a decrease in the amorphous layer thickness, as shown in Figure 7. This overall process is known as chemi-crystallization. This decrease in amorphous thickness can also describe the embrittlement of semi-crystalline polymers during aging [26]. It was previously shown that critical thickness exists [26] and can be defined as follows: when the amorphous layer thickness is above this critical value (l'_{ac}), the polymer exhibits ductile behavior, and when the amorphous layer thickness is below l'_{ac}, the polymer has brittle behavior.

Figure 16a shows the measured strain ratio as a function of the l_a value for the PE aged at the three temperatures considered in this study. It clearly appears that when the amorphous layer thickness exceeds 7.5 nm, the PE failure is ductile regardless of the aging condition (time or temperature). Conversely, when l_a is below 7.5 nm, then the polymer failure can be brittle. As a matter of fact, a critical layer thickness can be defined for the PE considered in this study about 7.5 nm.

To compare the values of l'_{ac} between the unimodal distribution and the initial bimodal distribution, it is necessary to use strain at break as the embrittlement criterion. According to Figure 16b, the data obtained here using a PE with an initial bimodal distribution of chain lengths is similar to that available in the literature for PE with a unimodal distribution. This suggests that this criterion can be used to describe embrittlement in PE, regardless of the initial distribution of the chain length.

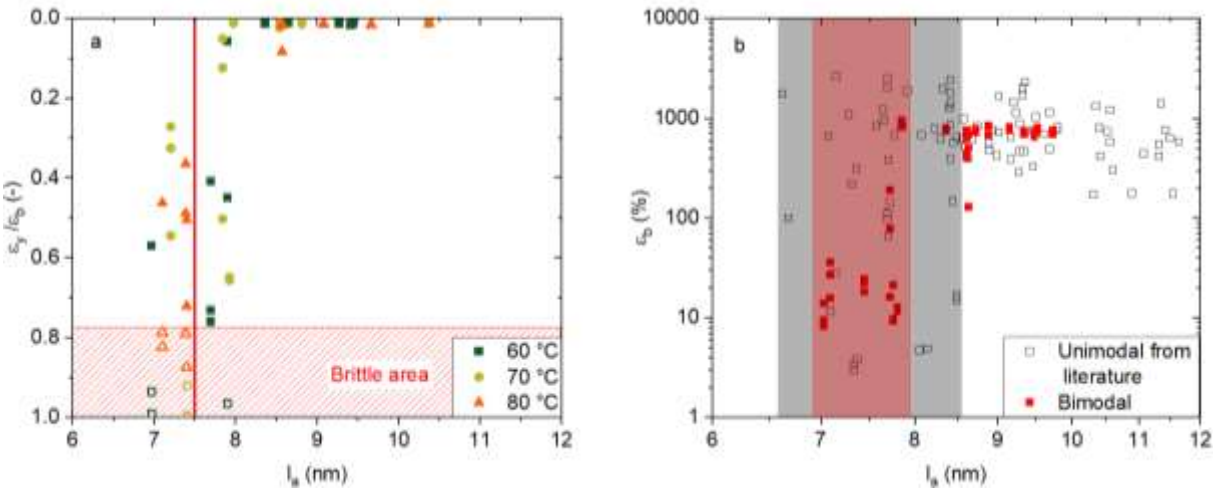

Figure 16: Determining the critical amorphous layer thickness (l'_{ac}) based on strain at break from this study (a) and comparisons with existing data from the literature[26] (b)

Finally, determining whether polymer embrittlement is caused by a decrease in the chain length or amorphous layer thickness is complex because these two factors are related [50]. Therefore, defining an embrittlement criterion based on physical considerations remains challenging. When comparing the results obtained from a bimodal chain length distribution with existing data on unimodal chain length distributions, it appears that the M'_c value differs for the two types of PE, whereas the l'_{ac} value remains the same. This suggests that embrittlement in semi-crystalline polymers is governed by the thickness of the amorphous layer. Although we lack solid evidence, this strong suggestion is a crucial step toward understanding polymer embrittlement during aging. It will require future studies to be confirmed.

Conclusions

PE with an initial bimodal chain length distribution (known as PE100-RC) was oxidized in air at three different temperatures (60 °C, 70 °C, and 80 °C). The material formulation and aging conditions were carefully selected to ensure homogeneous oxidation throughout the sample thickness and to keep the aging temperature below the melting process onset. Macromolecular characterizations were conducted to measure changes in the distribution of the chain length, the type and number of crystallites, and the thickness of the amorphous layer. Meanwhile, mechanical properties were determined using tensile tests.

This study found that during oxidation, the chain length distribution changed from bimodal to unimodal, which is a significant result. Meanwhile, oxidation caused an increase in crystallinity and a decrease in the thickness of the amorphous layer. In terms of mechanical behavior, the results indicated that oxidation caused the polymer to become brittle according to the embrittlement criterion based on the ratio between yield strain and strain at break established in this study. These findings are independent of the aging temperature range examined in this study.

Two distinct macromolecular embrittlement criteria can be defined for PE with an initial bimodal chain length distribution. Based on the molar mass of the polymer, if the PE has a molar mass above 100 kg/mol, it is ductile, whereas if M_w is below this value, it is brittle. This behavior is the same as for PE with a unimodal chain length distribution. However, based on existing data, the value of M'_c seems to

be higher for the PE considered here. The critical amorphous layer thickness (l'_{ac}) is found to be 7.5 ± 0.5 nm, which is similar to the existing value for unimodal PE in the literature.

The use of SEM micrographs of the sample surface obtained by electron backscatter diffraction can facilitate the completion of the understanding of the relationship between microstructure and embrittlement. This will enable the observation of the appearance of microcracks and crevices during aging, which can then be related to crystallite density.

Acknowledgements

The authors would like to acknowledge the work of Mickael Premel Cabic, Nicolas Lacotte, Otmane El Idrissi and Arnaud Le Moan. This work was supported by Électricité de France (EDF).

References

[1] The Freedonia Group, World Polyethylene, The Freedonia Group (2019). https://www.freedoniagroup.com/industry-study/world-polyethylene-3210.htm (accessed April 26, 2022).

[2] M. Amjadi, A. Fatemi, Creep behavior and modeling of high-density polyethylene (HDPE), Polymer Testing 94 (2021) 107031. https://doi.org/10.1016/j.polymertesting.2020.107031.

[3] R.K. Krishnaswamy, Analysis of ductile and brittle failures from creep rupture testing of high-density polyethylene (HDPE) pipes, Polymer 46 (2005) 11664–11672. https://doi.org/10.1016/j.polymer.2005.09.084.

[4] M. Schilling, U. Niebergall, M. Böhning, Full notch creep test (FNCT) of PE-HD – Characterization and differentiation of brittle and ductile fracture behavior during environmental stress cracking (ESC), Polymer Testing 64 (2017) 156–166. https://doi.org/10.1016/j.polymertesting.2017.09.043.

[5] H. Ben Hadj Hamouda, L. Laiarinandrasana, R. Piques, Viscoplastic behaviour of a medium density polyethylene (MDPE): Constitutive equations based on double nonlinear deformation model, International Journal of Plasticity 23 (2007) 1307–1327. https://doi.org/10.1016/j.ijplas.2006.11.007.

[6] C. Devilliers, L. Laiarinandrasana, B. Fayolle, E. Gaudichet-Maurin, Characterisation of aged HDPE pipes from drinking water distribution: investigation of crack depth by notched ring tests under creep loading, (n.d.).

[7] L. Hubert, L. David, R. Séguéla, G. Vigier, C. Corfias-Zuccalli, Y. Germain, Physical and mechanical properties of polyethylene for pipes in relation to molecular architecture. II. Short-term creep of isotropic and drawn materials, Journal of Applied Polymer Science 84 (2002) 2308–2317. https://doi.org/10.1002/app.10538.

[8] A. Lustiger, N. Ishikawa, An analytical technique for measuring relative tie-molecule concentration in polyethylene, Journal of Polymer Science Part B: Polymer Physics 29 (1991) 1047–1055. https://doi.org/10.1002/polb.1991.090290902.

[9] X. Lu, Z. Zhou, N. Brown, A sensitive mechanical test for slow crack growth in polyethylene, Polymer Engineering & Science 37 (1997) 1896–1900. https://doi.org/10.1002/pen.11839.

[10] A. Lustiger, R.L. Markham, Importance of tie molecules in preventing polyethylene fracture under long-term loading conditions, Polymer 24 (1983) 1647–1654. https://doi.org/10.1016/0032-3861(83)90187-8.

[11] A. Frank, I. Berger, F. Arbeiter, G. Pinter, Characterization of crack initiation and slow crack growth resistance of PE 100 and PE 100 RC pipe grades with Cyclic Cracked Round Bar (CRB) Tests, 2014. https://doi.org/10.13140/RG.2.1.4963.3688.

[12] L. Hubert, L. David, R. Séguéla, G. Vigier, C. Degoulet, Y. Germain, Physical and mechanical properties of polyethylene for pipes in relation to molecular architecture. I. Microstructure and crystallisation kinetics, Polymer 42 (2001) 8425–8434. https://doi.org/10.1016/S0032-3861(01)00351-2.

[13] P.J. DesLauriers, M.P. McDaniel, D.C. Rohlfing, R.K. Krishnaswamy, S.J. Secora, E.A. Benham, P.L. Maeger, A. r. Wolfe, A.M. Sukhadia, B.B. Beaulieu, A comparative study of multimodal vs. bimodal polyethylene pipe resins for PE-100 applications, Polymer Engineering & Science 45 (2005) 1203–1213. https://doi.org/10.1002/pen.20390.

[14] E. Nezbedova, G. Pinter, A. Frank, P. Hutar, J. Poduška, J. Hodan, Accelerated Tests for Lifetime Prediction of PE-HD Pipe Grades, Macromolecular Symposia 373 (2017) 1600096. https://doi.org/10.1002/masy.201600096.

[15] C. Long, Z. Dong, X. Liu, F. Yu, Y. Shang, K. Wang, S. Feng, X. Hou, C. He, Z.-R. Chen, Simultaneous enhancement in processability and mechanical properties of polyethylenes via tuning the molecular weight distribution from unimodal to bimodal shape, Polymer 258 (2022) 125287. https://doi.org/10.1016/j.polymer.2022.125287.

[16] Pipes | INEOS Olefins & Polymers Europe, (n.d.). https://www.ineos.com/businesses/ineos-olefins-polymers-europe/markets/construction-and-durables/pipes/ (accessed February 27, 2024).

[17] A.F. Reano, A. Guinault, E. Richaud, B. Fayolle, Polyethylene loss of ductility during oxidation: Effect of initial molar mass distribution, Polymer Degradation and Stability 149 (2018) 78–84. https://doi.org/10.1016/j.polymdegradstab.2018.01.021.

[18] J. Moreno, B. Paredes, A. Carrero, D. Vélez, Production of bimodal polyethylene on chromium oxide/metallocene binary catalyst: Evaluation of comonomer effects, Chemical Engineering Journal 315 (2017) 46–57. https://doi.org/10.1016/j.cej.2016.12.136.

[19] L.L. Bohm, H.F. Enderle, M. Fleißner, High-density polyethylene pipe resins, Advanced Materials 4 (1992) 234–238. https://doi.org/10.1002/adma.19920040317.
[20] C. Zou, Q. Wang, G. Si, C. Chen, A co-anchoring strategy for the synthesis of polar bimodal polyethylene, Nat Commun 14 (2023) 1442. https://doi.org/10.1038/s41467-023-37152-1.
[21] J. Cazenave, Sur le compromis rigidité / durabilité du Polyéthylène Haute Densité en relation avec la structure de chaîne, la microstructure et la topologie moléculaire issues de la cristallisation, These de doctorat, Lyon, INSA, 2005.
[22] H. Guo, R.G. Rinaldi, S. Tayakout, M. Broudin, O. Lame, The correlation between the mixed-mode oligo-cyclic loading induced mechanical and microstructure changes in HDPE, Polymer 224 (2021) 123706. https://doi.org/10.1016/j.polymer.2021.123706.
[23] B. Fayolle, L. Audouin, J. Verdu, Oxidation induced embrittlement in polypropylene — a tensile testing study, Polymer Degradation and Stability 70 (2000) 333–340. https://doi.org/10.1016/S0141-3910(00)00108-7.
[24] J. Tireau, L.V. Schoors, K. Benzarti, X. Colin, Environmental ageing of carbon black-filled polyethylene sheaths employed in civil engineering, (2009).
[25] S. Redjala, UV Aging Effects on Polycarbonate Properties, (2020).
[26] B. Fayolle, X. Colin, L. Audouin, J. Verdu, Mechanism of degradation induced embrittlement in polyethylene, Polymer Degradation and Stability 92 (2007) 231–238.
[27] M.A. Kennedy, A.J. Peacock, L. Mandelkern, Tensile Properties of Crystalline Polymers: Linear Polyethylene, Macromolecules 27 (1994) 5297–5310. https://doi.org/10.1021/ma00097a009.
[28] N. Khelidj, X. Colin, L. Audouin, J. Verdu, C. Monchy-Leroy, V. Prunier, Oxidation of polyethylene under irradiation at low temperature and low dose rate. Part II. Low temperature thermal oxidation, Polymer Degradation and Stability 91 (2006) 1598–1605. https://doi.org/10.1016/j.polymdegradstab.2005.09.012.
[29] P. Richters, Initiation Process in the Oxidation of Polypropylene, Macromolecules 3 (1970) 262–264. https://doi.org/10.1021/ma60014a027.
[30] L. Achimsky, L. Audouin, J. Verdu, Kinetic study of the thermal oxidation of polypropylene, Polymer Degradation and Stability 57 (1997) 231–240. https://doi.org/10.1016/S0141-3910(96)00167-X.
[31] R. Ferhoum, M. Aberkane, M. Ould Ouali, Distribution of nonliner relaxation (DNLR) approach of the annealing effects in semicristalline polymers: structure–property relation for high-density polyethylene (HDPE), Continuum Mech. Thermodyn. 26 (2014) 373–385. https://doi.org/10.1007/s00161-013-0306-9.
[32] ISO 11357-2, Analyse calorimétrique différentielle (DSC) — Partie 2: Détermination de la température et de la hauteur de palier de transition vitreuse, (2020).
[33] A. Peacock, Handbook of Polyethylene: Structures: Properties, and Applications, CRC Press, Boca Raton, 2014.
[34] B. Wunderlich, Macromolecular Physics: Crystal Melting, Academic Press, 2013.
[35] J.M. Haudin, A. Piana, B. Monasse, B. Gourdon, Étude des relations entre mise en forme, orientation et rétraction dans des films de polyéthylène basse densité réalisés par soufflage de gaine III. Orientation de la phase amorphe, Annales de Chimie Science Des Matériaux 25 (2000) 53–64. https://doi.org/10.1016/S0151-9107(00)88625-0.
[36] ISO 37 Caoutchouc vulcanisé ou thermoplastique — Détermination des caractéristiques de contrainte-déformation en traction, (2017).
[37] B. Fayolle, L. Audouin, J. Verdu, A critical molar mass separating the ductile and brittle regimes as revealed by thermal oxidation in polypropylene, Polymer 45 (2004) 4323–4330.
[38] M. Da Cruz, L. Van Schoors, K. Benzarti, X. Colin, Thermo-oxidative degradation of additive free polyethylene. Part I. Analysis of chemical modifications at molecular and macromolecular scales, Journal of Applied Polymer Science 133 (2016). https://doi.org/10.1002/app.43287.
[39] A. Holmström, E.M. Sörvik, Thermooxidative degradation of polyethylene. I and II. Structural changes occurring in low-density polyethylene, high-density polyethylene, and tetratetracontane heated in air, Journal of Polymer Science: Polymer Chemistry Edition 16 (1978) 2555–2586. https://doi.org/10.1002/pol.1978.170161012.
[40] X. Shi, J. Wang, S. Stapf, C. Mattea, W. Li, Y. Yang, Effects of thermo-oxidative aging on chain mobility, phase composition, and mechanical behavior of high-density polyethylene, Polymer Engineering & Science 51 (2011) 2171–2177. https://doi.org/10.1002/pen.21988.
[41] M. Iring, S. László-Hedvig, T. Kelen, F. Tüdós, L. Füzes, G. Samay, G. Bodor, Study of thermal oxidation of polyolefins. VI. Change of molecular weight distribution in the thermal oxidation of polyethylene and polypropylene, Journal of Polymer Science: Polymer Symposia 57 (1976) 55–63. https://doi.org/10.1002/polc.5070570107.
[42] L.E. Maley, Application of gel permeation chromatography to high and low molecular weight polymers, Journal of Polymer Science Part C: Polymer Symposia 8 (1965) 253–268. https://doi.org/10.1002/polc.5070080121.
[43] G. Meyerhoff, The efficiency of gel permeation chromatography, Journal of Polymer Science Part C: Polymer Symposia 21 (1968) 31–41. https://doi.org/10.1002/polc.5070210107.
[44] U.W. Gedde, M. Ifwarson, Molecular structure and morphology of crosslinked polyethylene in an aged hot-water pipe, Polymer Engineering & Science 30 (1990) 202–210. https://doi.org/10.1002/pen.760300403.
[45] N. Ladaci, Effet du Vieillissement et Analyse des Mécanismes du Comportement Mécanique et Tribologique d'un PEHD., Thesis, 2015. http://dspace.univ-guelma.dz/jspui/handle/123456789/338 (accessed April 6, 2022).
[46] M. Polińska, A. Rozanski, A. Galeski, J. Bojda, The Modulus of the Amorphous Phase of Semicrystalline Polymers, (2021).
[47] S. Humbert, O. Lame, G. Vigier, Polyethylene yielding behaviour: What is behind the correlation between yield stress and crystallinity?, Polymer 50 (2009) 3755–3761. https://doi.org/10.1016/j.polymer.2009.05.017.

[48] N. Brown, I.M. Ward, The influence of morphology and molecular weight on ductile-brittle transitions in linear polyethylene, J Mater Sci 18 (1983) 1405–1420. https://doi.org/10.1007/BF01111960.
[49] M. Da Cruz, Approche multi-échelle du vieillissement thermo-oxydatif du polyéthylène utilisé dans les applications de génie civil et de BTP, (2015) 213.
[50] B. Fayolle, E. Richaud, X. Colin, J. Verdu, Review: degradation-induced embrittlement in semi-crystalline polymers having their amorphous phase in rubbery state, J Mater Sci 43 (2008) 6999–7012. https://doi.org/10.1007/s10853-008-3005-3.

Declaration of interests

☒ The authors declare that they have no known competing financial interests or personal relationships that could have appeared to influence the work reported in this paper.

☐ The authors declare the following financial interests/personal relationships which may be considered as potential competing interests: